The Approach of a Neuron Population Firing Rate to a New Equilibrium: An Exact Theoretical Result

B. W. Knight
Rockefeller University, New York, NY 10021, and Laboratory of Applied Mathematics, Mount Sinai School of Medicine, New York, NY 10029, U.S.A.

A. Omurtag
Laboratory of Applied Mathematics, Mount Sinai School of Medicine, New York, NY 10029, U.S.A.

L. Sirovich
Rockefeller University, New York, NY 10021, and Laboratory of Applied Mathematics, Mount Sinai School of Medicine, New York, NY 10029, U.S.A.

The response of a noninteracting population of identical neurons to a step change in steady synaptic input can be analytically calculated exactly from the dynamical equation that describes the population's evolution in time. Here, for model integrate-and-fire neurons that undergo a fixed finite upward shift in voltage in response to each synaptic event, we compare the theoretical prediction with the result of a direct simulation of 90,000 model neurons. The degree of agreement supports the applicability of the population dynamics equation. The theoretical prediction is in the form of a series. Convergence is rapid, so that the full result is well approximated by a few terms.

1 Introduction and Results

A population-dynamics approach has been introduced as a means for the efficient simulation of the activity of large neuron populations (Knight, Manin, & Sirovich, 1996). Recent studies support and verify the power of this new approach (Omurtag, Knight, & Sirovich, 2000; Sirovich, Knight, & Omurtag, forthcoming; Nykamp & Tranchina, 2000). A general treatment of this approach with further analytic exploration appears in Knight (2000). In this article we follow up on one such feature.

It is commonly the case that a dynamical system, which is not disturbed by any time-varying external inputs, will possess a time-independent equilibrium configuration. It also is typically the case that when a dynamical system is in a state near—but not at—that equilibrium, we may describe the early evolution of its subsequent motion in terms of the changing amplitudes of a set of normal modes that in effect impose a privileged set of

coordinates on the system's state-space in the neighborhood of the equilibrium point. Normal modes come as either singles, whose amplitudes change exponentially with time, or natural pairs, whose coordinated amplitudes change together in time as sine and cosine multiplied by an envelope that changes exponentially with time. An arbitrary initial condition near equilibrium will yield a time evolution that is a superposition of these motions.

The dynamical equation that describes the time evolution of a noninteracting neuron population density conforms to the general rule just quoted. However, there is an important additional feature: because the neurons are noninteracting, superposition of component probabilities is respected by the time evolution of their density function, and so the dynamical equation is linear in the population density. Because of this, the general rule quoted above is *exact* for the population dynamics equation: the rule describes the nature of our system's evolution toward equilibrium even if we do not confine our initial condition to the neighborhood of the equilibrium point.

If the neuron population receives an input signal that is time independent at one value and then jumps abruptly to a new value, where it holds steady again, the prejump equilibrium point becomes a specific postjump nonequilibrium point from which the system will proceed to evolve to the new equilibrium point in accordance with our rule, and the transient response of the population firing rate will reflect this dynamics. All of this we have reasoned out here without so far having to define a specific neuron model and without having to turn to any explicit mathematics. To proceed to quantitative predictions, we must have an explicit neuronal model and, from the dynamical equation for its population density, calculate the following things:

1. The equilibrium points before and after the jump in input.

2. The normal modes for the postjump equilibrium point, and their characteristic exponential decay rates and sinusoidal frequencies.

3. The coefficients that express the prejump equilibrium point as a superposition of those normal modes.

4. As the calculations above yield an explicit expression for the population density's time course, all that remains is to express the population firing rate in terms of that density.

The result of these steps is an explicit expression (Knight, 2000) stating that under common circumstances, the new equilibrium firing rate is approached with a time course that is an exponentially decaying sinusoid, whose oscillation rate is near to the single-neuron firing rate at the new equilibrium.

We compare the analytic result with a direct simulation of a population of 90,000 neurons. These are integrate-and-fire neurons with firing threshold
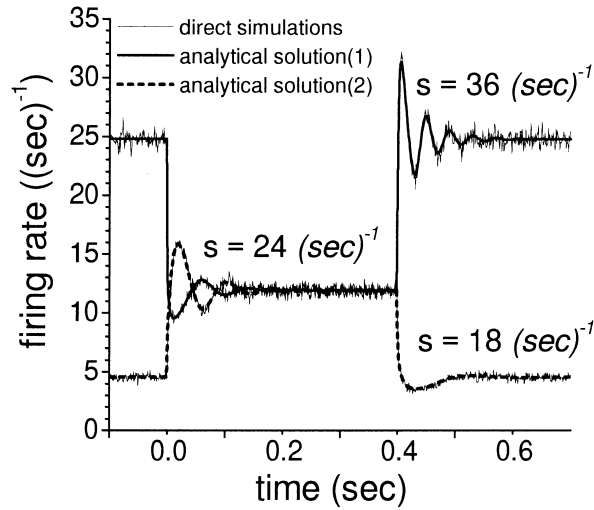
Figure 1: Prediction of simulation results by theory. A population of 90,000 neurons was simulated and per-neuron firing rate (irregular thin line) calculated from impulses in each millisecond. Theoretical equilibrium levels are 4.54, 11.92, 24.79 sec^{-1}. For comparison, the damped transients have theoretical principal-mode frequencies of 5.77, 11.50, 24.70 sec^{-1}.

voltage scaled to unity, with an ohmic shunt that gives a decay rate constant of $\gamma = 20\,\text{sec}^{-1}$, and for which each synaptic event advances the dimensionless scaled voltage variable toward threshold by an instantaneous step of $h = .03$. These nominal values are representative of realistic measures. The input to each neuron is a Poisson process with a common specified mean rate. To simplify comparison with the more familiar nonstochastic limit ($h \to 0$) it is more convenient to specify the scaled mean input *current* $s\,(\text{sec}^{-1})$ which is the mean input rate times the synaptic step h. (In the nonstochastic limit and without ohmic leakage, s would be equal to the neuron firing rate; however, with the presence of ohmic leakage, the nonstochastic neuron's firing rate drops to zero when s is moved to less than γ. For large s, the firing rate of the nonstochastic neuron with leakage approaches $s - \frac{1}{2}\gamma$ from below. The following section furnishes some theoretical details.)

Figure 1 shows the results of four direct simulation numerical experiments in which s is jumped to the three steady values 18, 24, 36 sec^{-1} and the firing rates find equilibrium at 4.54, 11.92, 24.79 sec^{-1}. The larger two values are not far below their nonstochastic-and-large-s estimated values $\left(s - \frac{1}{2}\gamma\right)$ of 14 and 26 sec^{-1}. However the lowest input $\left(s = 18\,\text{sec}^{-1} < \gamma = 20\,\text{sec}^{-1}\right)$ is below the corresponding nonstochastic firing threshold, and the firing that we see depends on unusually closely spaced clusters of synaptic events

which are permitted by the Poisson arrival statistics. In Figure 1, for graphic presentation the neuron firings have been averaged over 1 millisecond bins.

The transients that lead to equilibrium in Figure 1 convey further information. In each case the exact analytical solution is given by the smooth line, which passes centrally through the slightly noisy direct simulation result. There is no indication of any systematic departure of the exact analytical solution from the results of the direct simulation.

In each of the four cases, after a fraction of a cycle, the return of the transient to equilibrium takes the form of a damped sinusoid. Although it is hard to see in the highly damped case of the lowest equilibrium firing rate, in each case the frequency of the sinusoid lies close to the mean firing rate at equilibrium.

In Figure 1, the amplitude of the residual noise in the simulation results is inversely proportional to the square root of the number of neurons simulated. We see that to approach the precision of the theoretical curves, simulation of about 9 million neurons would be required.

2 Some Further Theoretical Details

The exact analytical solution of the return-to-equilibrium problem follows directly from the general population dynamics theory and has been presented in some detail in Knight (2000). Here we give a brief general development and then discuss the specifics of the case that was used in the simulation.

The momentary state of a model neuron is specified by values of internal variables such as its transmembrane potential and the channel variables that determine its various transmembrane ionic conductances. The neuron's state may be thought of as a point in a state-space in which the possible values of the internal variables specify a coordinate system. As time advances, the neuron's point in the state-space moves in accordance with a specified dynamics. A set of similar neurons corresponds to a set of points, and typically their motions will depend on a mean external input s, which they share in common, and also on stochastic inputs, which they receive independently. The momentary state of a large population of similar neurons can be described by a *population density* ρ, which specifies the likelihood that a neuron blindly picked at random will be found in the vicinity of any specified point in the state-space. The population density thus integrates to unity. It evolves in time in accordance with a dynamical equation of the general form

$$\partial\rho/\partial t = Q(s)\rho, \tag{2.1}$$

where the right-hand side is specified by the law of motion of the individual neurons and is a function, over the state-space, that depends linearly on ρ. Thus $Q(s)$ is technically a linear operator, which depends on the common input s.

In our situation, s remains fixed after an abrupt jump. In this circumstance it is a generic property (essentially a commonly occurring feature) of linear operators that in the state-space we can find a set of eigenfunctions, ϕ_n, such that the action of the linear operator on these is simply to multiply by an eigenvalue λ_n according to the relation

$$Q\phi_n = \lambda_n\phi_n. \tag{2.2}$$

The eigenfunctions have the further important property that any function in the state-space may be expressed as a weighted sum of them. In particular we can do this for the population density ρ, though we must observe that ρ evolves in time according to equation 2.1, and so the weightings in its eigenfunction sum must evolve as well. Equation 2.1 in fact demands that ρ must be of the form

$$\rho = \sum_n a_n e^{\lambda_n t}\phi_n. \tag{2.3}$$

Substitute equation 2.3 in 2.1. Perform the time differentiation on the left, and use equation 2.2 on the right to confirm that 2.3 is indeed a solution. Below we will see that a few terms of equation 2.3 furnish a close approximation to the full sum.

Now equation 2.1 has an equilibrium solution that is independent of time. From either equation 2.1 or 2.3, the equilibrium solution is clearly an eigenfunction ϕ_0 of equation 2.2 with the eigenvalue

$$\lambda_0 = 0. \tag{2.4}$$

(See Sirovich et al., forthcoming, for a general treatment of the equilibrium problem.)

From equation 2.3, we note that all the other eigenfunctions have the properties that were discussed in Section 1 as the properties of normal modes. In fact the eigenvalues λ_n of equation 2.2 typically will be complex numbers with negative real parts and which arise in complex conjugate pairs. It is convenient to assign integers to them in the order of increasing negativity of their real part, and corresponding negative integers to those eigenvalues that are the complex conjugates of eigenvalues whose imaginary parts are positive. The eigenfunctions typically will be complex and occur in conjugate pairs; similarly their coefficients in the sum for ρ, equation 2.3, will be complex conjugates, so that the sum breaks up into natural pairs of terms. Each pair is real, and as the time t advances, the nth pair decrements exponentially and oscillates sinusoidally according to the rate and the radian frequency, which are expressed by the real and imaginary parts of the nth eigenvalue.

To determine the population density ρ, we have still to evaluate the constants a_n in equation 2.3. If we set t to zero in equation 2.3, the summation

must give us the equilibrium distribution of the population density *before* the input s underwent its abrupt jump. Let us call this equilibrium density $\phi_0^{(-)}$; we must expand it in terms of the eigenfunctions *after* the jump.

Pairs of complex-valued functions that are supported by our state-space have a natural bilinear inner product. If $\mathbf{x}$ denotes a point in the state-space, and $v(\mathbf{x})$ and $u(\mathbf{x})$ are functions, their natural inner product is

$$(v, u) = \int d\mathbf{x} \, (v(\mathbf{x}))^* u(\mathbf{x}), \tag{2.5}$$

where the integral extends over the state-space. The set of eigenfunctions from equation 2.2 determines a companion set $\widehat{\phi}_n$ of biorthonormal functions that satisfy the inner product relations,

$$\left(\widehat{\phi}_m, \phi_n\right) = \delta_{mn}, \tag{2.6}$$

where δ_{mn} is unity if $m = n$ and zero otherwise. This biorthonormal set are determined by equation 2.6 and may be constructed from the ϕ_n by straightforward procedures of linear algebra. Alternatively, if equation 2.1 is discretized for computational purposes, standard software will compute the $\widehat{\phi}_n$ as the eigenvectors of the matrix transpose of Q.

If t is set to zero in equation 2.3, we have

$$\phi_0^{(-)} = \sum_n a_n \phi_n. \tag{2.7}$$

With a prejump steady-state distribution $\phi_0^{(-)}$ on hand, we may evaluate the as-yet-unknown coefficients a_n by

$$a_m = \left(\widehat{\phi}_m, \phi_0^{(-)}\right); \tag{2.8}$$

if we substitute equation 2.7 into 2.8 and use 2.6, we confirm 2.8 as an identity. The postjump time course of ρ, given by equation 2.3, now is fully evaluated.

The methodology just reviewed is classical. Stability near equilibrium in nonlinear systems is extensively discussed by Iooss and Joseph (1980). The eigenvalue theory of linear operators, with applications, is discussed in much detail by Morse and Feshbach (1953) and more briefly by Page (1955).

To find the time course of the population firing rate, as implied by the dynamics that we have solved, we need some further structure of our neuron model. As we follow the trajectory of a neuron in its state-space, at some point on that trajectory we can say that the neuron has just fired an impulse. As we look at the set of all trajectory lines, each has a firing point. The rate (on a per-neuron basis) at which the noninteracting neurons of a large population pass their firing points must depend in a linear way on the population density function. We may write

$$r = R\{\rho\}; \tag{2.9}$$

the firing rate r is a linear functional of the population density ρ. If we substitute ρ from equation 2.3 into 2.9, we obtain

$$r(t) = \sum_n a_n e^{\lambda_n t} R\{\phi_n\}$$

$$= \sum_n \left(\widehat{\phi}_n, \phi_0^{(-)}\right) R\{\phi_n\} e^{\lambda_n t}. \qquad (2.10)$$

Once we have the prejump equilibrium distribution, the postjump eigenfunctions and eigenvalues and the firing-rate linear functional, this is an explicit and exact evaluation. Equation 2.10 was used to calculate the smooth lines in Figure 1.

The neurons in our simulation follow the dynamical equation,

$$dx/dt = -\gamma x + \sum_n h\delta(t - t_n), \qquad (2.11)$$

where x is the dimensionless voltage, and the synaptic input times, t_n, are drawn from a Poisson process with mean rate s/h, and are independently chosen for each neuron. When a synaptic input jumps a neuron beyond $x = 1$, the neuron is reset to $x = 0$ and a nerve impulse is registered. If we hold s fixed and let h go to zero, equation 2.11 goes to

$$dx/dt = -\gamma x + s, \qquad (2.12)$$

which is the familiar equation for the forgetful or "leaky" integrate-and-fire neuron. We note that if γ is larger than s, then

$$x = s/\gamma \qquad (2.13)$$

gives an equilibrium solution to equation 2.12 that is below the firing threshold. Equation 2.12 may be rearranged to the form

$$dt = dx/(s - \gamma x) \quad \text{or}$$

$$T = \int_0^1 dx/(s - \gamma x) = -\frac{1}{\gamma} \ln\left(1 - \frac{\gamma}{s}\right) \qquad (2.14)$$

for the firing period, unless small s makes s/γ less than unity. The firing rate is the reciprocal firing period

$$r = 1/T \to s - \frac{1}{2}\gamma \quad \text{for large } s, \qquad (2.15)$$

as mentioned in section 1.

The dynamical equation for the population density that follows from equation 2.11 is

$$\frac{\partial \rho\left(x, t\right)}{\partial t} = \frac{\partial}{\partial x}\left[\gamma x \rho\left(x, t\right)\right] + \frac{s}{h}\left[\rho\left(x - h, t\right) - \rho\left(x, t\right)\right]. \tag{2.16}$$

The first right-hand term corresponds to backward advective drift in voltage as the current γx leaks back through the ohmic shunt; the second term (absent if $x < h$) corresponds to density accumulation as neurons jump in from voltage $x - h$. The third term similarly corresponds to density depletion as neurons jump away from the voltage x. The s-dependent right-hand side expresses a linear transformation upon ρ, and so defines the linear operator $Q\left(s\right)$ in equation 2.1 for this particular case. Equation 2.16 was studied by Wilbur and Rinzel (1982) and in further detail by Omurtag et al. (2000), and Sirovich et al. (forthcoming). As shown in Omurtag et al. (2000), equation 2.16 follows rigorously from equation 2.11 and the Poisson specification of synaptic input times, without introduction of free parameters.

(If in equation 2.16 we were to expand the term that is offset in h, as a Taylor series in h, and keep terms through h^2, we would reduce the equation to a second-order partial differential equation that describes the dynamics of the probability density in terms of advection and diffusion in state-space. Such an approximate dynamical equation for the probability density is technically known as a Fokker-Planck equation and is extensively discussed by Risken, 1996. Application of the Fokker-Planck equation to the integrate-and-fire neuron model is discussed by Tuckwell, 1988.)

The population firing rate linear functional $R\{\rho\}$ in the present case is the rate at which neurons make a final synaptic jump that carries them beyond $x = 1$. It is proportional to the synaptic rate s/h and also clearly depends equally on $\rho\left(x\right)$ for all values of x larger than $1 - h$. It is

$$r\left(t\right) = R\left\{\rho\right\} = \frac{s}{h}\int_{1-h}^{1} dx \rho\left(x, t\right). \tag{2.17}$$

The specific case of the eigenvalue equation, 2.2, which corresponds to the dynamical equation, 2.16, is

$$\frac{d}{dx}\left[\gamma x \phi_n\left(x\right)\right] + \frac{s}{h}\left[\phi_n\left(x - h\right) - \phi_n\left(x\right)\right] = \lambda_n \phi_n\left(x\right). \tag{2.18}$$

We have discretized this equation into 200 compartments. We have discretized equation 2.17, which serves as the input into the first compartment of the discretized equation, 2.18. The resulting system we have solved for its eigenvalues and eigenfunctions. These compare well with corresponding
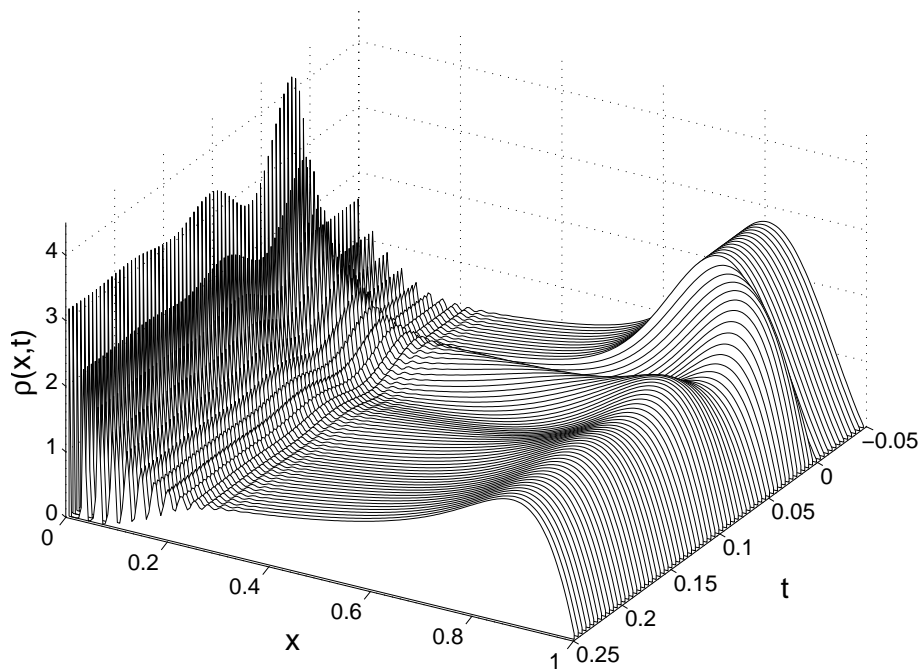
Figure 2: Evolution of the population density following a change of mean input current from $18\,\mathrm{sec}^{-1}$ to $24\,\mathrm{sec}^{-1}$.

eigenvalues and eigenfunctions obtained by approximate analytic methods (Omurtag et al., 2000; Sirovich et al., forthcoming). These eigenvalues and eigenfunctions (including $\phi_0^{(-)}$) and the discretized evaluation of $R\{\phi_n\}$ from equation 2.17 have been used in equation 2.10 in order to calculate the smooth lines in Figure 1.

Figure 2 gives a perspective view of the evolution of the population density, as time advances from the back of the figure toward the viewer, in the case where the average current suddenly shifts from its lowest setting of $18\,\mathrm{sec}^{-1}$ up to $24\,\mathrm{sec}^{-1}$. Initially the population density is mostly concentrated in the upper end of the range, where forward jumping and backward advection approximately balance. With the onset of more frequent forward jumping, at time $t = 0$, this accumulation is swept away and is returned to the low-voltage region. Then it is swept forward as it disperses and arrives once more at the high-voltage end after about $1/10$ sec, which is consistent with the new single-neuron firing rate of $11.92/\,\mathrm{sec}$. We are able to follow this still-dispersing concentration through about one additional round trip,
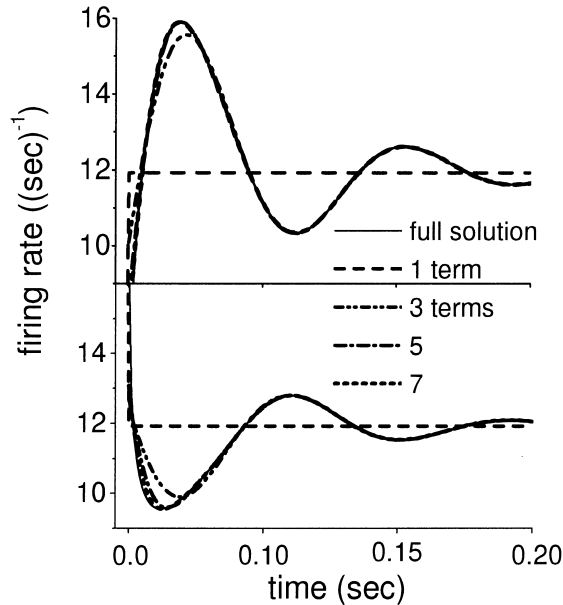
Figure 3: Convergence of partial sums to the full theoretical result.

consistent with the corresponding firing response in Figure 1, which goes through about two visible decrementing oscillations.

The high peaks of probability concentration at low voltages arise because of the discrete voltage jump of $h = .03$, and wash out because the irregularly timed jumping is not synchronized with the steady advective backward drift, which is due to capacitor-discharge as ohmic current leaks through the model nerve membrane. The choice above of 200 voltage divisions for the numerical work was made to resolve these peaks adequately in the population density.

Figure 3 addresses the convergence of the series in equation 2.10. For the case of $s = 24 \sec^{-1}$, we plot the partial sums for both the ascending and descending transients. After the second passage across the equilibrium value, the first pair of eigenfunctions yields an accurate description of the transient in both cases. Between the first and second passage, the descending transient is fairly well fit by two pairs of eigenfunctions, while four pairs give a result indistinguishable from the full result. For the ascending transient in the same span, only two pairs are needed to replicate the full solution visually. In summary, we see that the exact analytic solution for the transient to a new equilibrium accounts well for the results of the direct simulation, and after the first equilibrium crossing, the full analytic result is excellently approximated by a short, truncated sum that may be expressed in terms of a few parameters.

The manner in which this same sort of treatment may be applied to more detailed neuron models, such as that of Hodgkin and Huxley (1952), is given some discussion in Knight (2000). The effect of feedback (where the output contributes to the input and the population dynamics consequently becomes nonlinear in the population density) is also discussed in Knight, and with a somewhat different emphasis in Sirovich et al. (forthcoming). These publications are available at our web site.

Acknowledgments

References

Hodgkin, A. L., & Huxley, A. F. (1952). A quantitative description of membrane current and its application to conduction and excitation in nerve. *J. Physiol.*, *117*, 500–544.

Iooss, G., & Joseph, D. D. (1980). *Elementary stability and bifurcation theory*. New York: Springer-Verlag.

Knight, B. W. (2000). Dynamics of encoding in neuron populations: Some general mathematical features. *Neural Computation, 12*, 497–542.

Knight, B. W., Manin, D., & Sirovich, L. (1996). Dynamical models of interacting neuron populations. In E. C. Geil (Ed.), *Symposium on Robotics and Cybernetics: Computational Engineering in Systems Applications*. Lille, France: Cite Scientifique.

Morse, P. M., & Feshbach, H. (1953). *Methods of theoretical physics*. New York: McGraw-Hill.

Nykamp, D., & Tranchina, D. (2000). A population density approach that facilitates large-scale modeling of neural networks: Analysis and an application to orientation tuning. *J. Comp. Neurosci., 8*, 19–50.

Omurtag, A., Knight, B. W., & Sirovich, L. (2000). On the simulation of large populations of neurons. *J. Comp. Neurosci., 8*, 51–63.

Page, C. H. (1955). *Physical mathematics*. New York: Van Nostrand.

Risken, H. (1996). *The Fokker-Planck equation: Methods of solution and applications*. New York: Springer-Verlag.

Sirovich, L., Knight, B. W., & Omurtag, A. (Forthcoming). Dynamics of neuronal populations: The equilibrium solution. *SIAM*.

Tuckwell, H. C. (1988). *Introduction to theoretical neurobiology* (Vol. 2). Cambridge: Cambridge University Press.

Wilbur, W. J., & Rinzel, J. (1982). An analysis of Stein's model for stochastic neuronal excitation. *Biological Cybernetics*, *45*, 107–114.